Journal of
Cardiovascular Development and Disease

MDPI

Review

Novel CMR Indices of Cardiac Function and Remodeling in Right Heart Disease

Edmund Naami [1,†], Ana Pastorino [2,†], Robert S. Zhang [1], Elizabeth Manowitz [1], Jonathan W. Weinsaft [1], Jiwon Kim [1] and Omar K. Khalique [2,*]

[1] Division of Cardiology, Weill Cornell Medical Center, New York, NY 10065, USA; edn4002@med.cornell.edu (E.N.)
[2] Division of Cardiovascular Imaging, St. Francis Hospital & Heart Center, Roslyn, NY 11576, USA; ana.pastorino@chsli.org
* Correspondence: omar.khalique@chsli.org
† These authors contributed equally to this work.

Abstract

Right ventricular (RV) remodeling is an important determinant of prognosis in conditions marked by chronic RV volume or pressure overload, including functional tricuspid regurgitation (TR) and pulmonary hypertension (PH). Conventional volumetric and functional measures, including RV ejection fraction (RVEF), often fail to detect adverse remodeling until it is advanced, particularly in significant TR, where regurgitant flow inflates total stroke volume and can mask a reduction in effective forward output. Cardiac magnetic resonance (CMR) is well suited to address this gap, combining highly reproducible chamber quantification with novel measures of myocardial deformation, tissue characterization, RV–pulmonary artery (PA) interaction, and flow hemodynamics. This narrative review examines emerging CMR-derived indices of adverse right heart remodeling, including effective RVEF, the RV/left ventricular volume ratio, the right atrioventricular coupling index, nonischemic septal fibrosis, and hepatic extracellular volume (ECV). We further review functional CMR markers, including surrogates of RV-PA coupling, RV and right atrial strain, myocardial T1 and ECV mapping, markers of treatment response and reverse remodeling, and 4D-flow assessment of PA hemodynamics. For each, we discuss underlying physiology, supporting data, proposed clinical thresholds, and current barriers to clinical adoption, and we compare the maturity of the supporting evidence across indices. Collectively, these indices represent a shift toward physiologically based, mechanism-specific risk stratification in right heart disease and may help identify patients at risk for adverse outcomes before conventional volumetric or functional parameters decline. However, their supporting evidence varies considerably in maturity, proposed thresholds are population- and methodology-dependent, and whether their use improves the timing of intervention or patient outcomes remains to be established in prospective studies.

Keywords: CMR indices; right heart disease; prognostication; right-heart remodeling

Check for updates

Academic Editor: Zhonghua Sun

Received: 30 September 2026
Revised: 23 October 2026
Accepted: 26 October 2026
Published: 30 October 2026

Copyright: © 2026 by the authors. Licensee MDPI, Basel, Switzerland. This article is an open access article distributed under the terms and conditions of the Creative Commons Attribution (CC BY) license.

1. Introduction

The right ventricle (RV) undergoes both structural and functional adaptations in response to chronic pressure or volume overload, collectively termed RV remodeling [1]. Chronic RV pressure overload typically induces an initial phase of concentric hypertrophy, whereas chronic RV volume overload characteristically leads to eccentric dilation, although in advanced disease these patterns frequently coexist. These changes occur at the

cardiomyocyte, extracellular matrix, and chamber levels, and determine whether the RV maintains adequate cardiac output or progresses to failure [1]. Early in the disease course, the RV may compensate for increased afterload via concentric hypertrophy and enhanced contractility. These adaptations help preserve the coupling between RV contractility and pulmonary artery afterload (i.e., RV-PA coupling) [2]. Ultimately, these compensatory adaptations fail, leading to RV-PA uncoupling and subsequent RV dilation with progressive functional impairment [1,2]. Physiologically, RV failure reflects an accumulation of adverse processes including maladaptive structural remodeling, neurohormonal overactivation, and myocardial fibrosis [3].

Studies demonstrate that the occurrence of RV dysfunction is substantial. A recent large single-center echocardiographic cohort estimated the incidence of new RV dysfunction at 8.2% [4]. In the community-based elderly ARIC cohort, abnormal right ventricular ejection fraction was present in roughly 15% of participants at stage A heart failure and 24% at stage B, with even higher prevalence among those with stage C heart failure [5]. Furthermore, a systematic review and meta-analysis of 38 studies in patients with heart failure with preserved ejection fraction (HFpEF) found RV dysfunction by tricuspid annular plane systolic excursion (TAPSE) in 28% of patients, and by fractional area change in 18% [6]. Beyond this considerable burden, RV dysfunction is far from an incidental structural finding, as it carries substantial prognostic weight. In the CMR-based Multi-Ethnic Study of Atherosclerosis (MESA), abnormal RV structure was associated with more than double the risk of subsequent heart failure or cardiovascular death [7]. Taken together, these data indicate that RV remodeling is neither rare nor limited to end-stage disease, but rather a common and prognostically consequential process across the spectrum of cardiovascular disease.

Among the many causes of RV dysfunction, pulmonary hypertension (PH) and tricuspid regurgitation (TR) are two of the most extensively studied, representing the chronic pressure- and volume-overload states, respectively, that are the focus of this review. A recent large hospital-based cohort study of 22,317 adults undergoing echocardiography found clinically significant TR in 10.3% of the overall population [8]. Pulmonary hypertension, meanwhile, remains a common driver of RV pressure overload, and global estimates for pulmonary arterial hypertension (PAH) alone place the 2021 prevalence near 192,000 cases with over 22,000 associated deaths, with both prevalence and incidence projected to rise further as populations age [9].

Given that RV maladaptation dictates prognosis in both TR and PH, early detection of adverse remodeling beyond changes in conventional volumetric and functional indices has become a central goal of contemporary right-heart imaging. CMR is well suited to this purpose, combining highly reproducible chamber quantification with novel measures of myocardial deformation, tissue characterization, RV–PA interaction, and pulmonary flow hemodynamics. This review examines novel CMR-derived indices and functional CMR markers of adverse right-heart remodeling, with particular emphasis on their mechanistic basis, prognostic value, maturity of supporting evidence, and potential for clinical translation.

This is a narrative review. The relevant literature was identified through a search of PubMed without restriction on publication date, using broad combinations of terms related to CMR ("cardiac magnetic resonance," "cardiovascular magnetic resonance," "CMR," "cardiac MRI"), the right heart ("right ventricle," "right ventricular function," "right ventricular remodeling," "right atrium," "right atrial function," "right heart," "ventricular interdependence," "RV-PA coupling"), the clinical conditions of interest ("tricuspid regurgitation," "functional tricuspid regurgitation," "secondary tricuspid regurgitation," "pulmonary hypertension," "pulmonary arterial hypertension," "chronic thromboembolic pulmonary hypertension"), specific indices and techniques ("ejection fraction," "effective ejection fraction," "volume ratio," "atrioventricular coupling," "late gadolinium enhance-

ment," "fibrosis," "T1 mapping," "extracellular volume," "hepatic," "liver," "strain," "feature tracking," "phase contrast," "4D flow," "wall shear stress," "vortex"), and outcomes ("prognosis," "mortality," "outcome," "risk stratification," "treatment response," "reverse remodeling," "transcatheter tricuspid intervention"). Reference lists of relevant original articles and reviews were also screened, and the search was supplemented by the authors' knowledge of the field, including studies from their own research group. We prioritized original studies in adults with functional TR or PH that reported CMR-derived right-heart indices in relation to clinical outcomes, invasive hemodynamics, or treatment response, with particular attention to larger, more recent, and multicenter cohorts. Case reports and studies without CMR data were not included. Consistent with the narrative design, no formal risk-of-bias assessment or quantitative synthesis was performed, and study selection may be subject to selection bias.

2. Novel CMR-Based Indices

Several novel CMR-indices have emerged to characterize complementary aspects of right-heart remodeling and provide incremental prognostic information (Table 1). The study populations, proposed thresholds and their derivation, endpoints, and validation status of these indices are compared in Table 2.

2.1. Effective RVEF

Effective right ventricular ejection fraction (eRVEF) is a CMR-derived index designed to provide a more accurate assessment of effective forward RV performance in the presence of significant tricuspid regurgitation. Rather than being calculated from total RV stroke volume, eRVEF is defined as the ratio of forward stroke volume, the blood volume actually propelled into the pulmonary circulation, to RV end-diastolic volume (Figure 1A–E) [10].

The physiologic rationale follows directly from a limitation inherent to conventional RVEF in significant TR, where total RV stroke volume comprises both the forward volume ejected into the pulmonary artery and the regurgitant volume that flows backward into the right atrium. In TR, the regurgitant flow inflates total stroke volume and, with it, conventional RVEF, even as effective forward output declines. RV function can therefore appear preserved or only mildly reduced by conventional RVEF after meaningful myocardial deterioration has occurred, an effect directly analogous to how left ventricular (LV) ejection fraction (LVEF) is falsely reassuring in significant mitral regurgitation. By restricting the numerator to forward volume, eRVEF removes this regurgitant inflation and more directly reflects the RV's effective forward output [10].

Importantly, eRVEF should be interpreted as a measure of effective forward pumping performance in the presence of TR rather than as a direct measure of intrinsic RV myocardial contractility. Like conventional RVEF, it remains load-dependent and is influenced by RV preload and pulmonary vascular afterload. Its accuracy also depends on pulmonary artery phase-contrast flow quantification, which may be affected by arrhythmia, irregular RR intervals, and background phase-offset errors. In addition, conditions that alter net pulmonary forward flow independently of TR, such as significant pulmonary regurgitation or intracardiac shunting, may confound its interpretation.

A recent validation study evaluated eRVEF in a derivation cohort of 453 patients with at least moderate functional TR (regurgitant fraction $\geq$ 30% or regurgitant volume $\geq$ 30 mL) undergoing CMR, and identified a threshold of eRVEF $\leq$ 25% derived from all-cause mortality data [10]. Additionally, eRVEF was associated with advanced biventricular remodeling and biventricular dysfunction. After adjusting for conventional TR prognostic markers including TR severity, RV size, and conventional RVEF, eRVEF remained independently predictive of mortality. In model comparisons, adding eRVEF to a model that already

included conventional RVEF significantly improved mortality prediction, whereas adding conventional RVEF to a model that already included eRVEF did not meaningfully improve prediction, indicating that eRVEF provides incremental prognostic value over conventional RVEF [10]. The ≤25% threshold was subsequently tested in two independent external cohorts from separate institutions (combined $n = 316$), in which it remained prognostically significant (hazard ratio [HR] 2.66–2.86) [10]; among the indices reviewed here, eRVEF is the only one whose proposed threshold has been tested in independent external cohorts. Nonetheless, all cohorts were observational, the threshold was derived and tested exclusively in functional TR and has not been evaluated in PH or other right-heart diseases, and prospective validation is lacking.

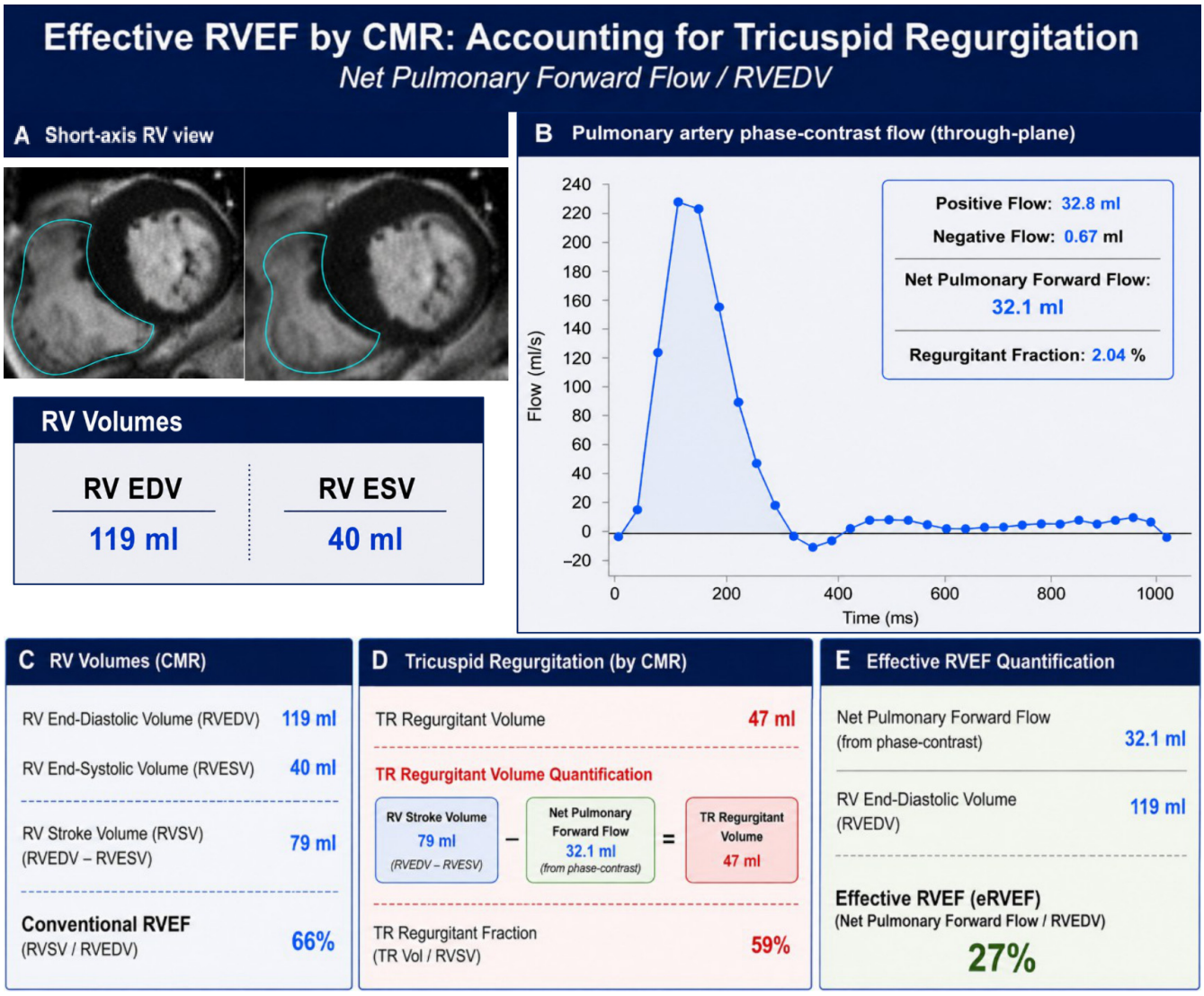


Figure 1. Effective right ventricular ejection fraction by cardiovascular magnetic resonance accounting for tricuspid regurgitation. (**A**) Short-axis cine CMR. End-diastolic and end-systolic right ventricular contours for volumetric assessment. Green lines indicate the RV endocardial contours. (**B**) Pulmonary artery phase-contrast CMR. Through-plane flow quantification provides net pulmonary forward flow. (**C**) Right ventricular volumetric assessment. Right ventricular end-diastolic and end-systolic volumes are used to derive stroke volume and conventional RVEF. (**D**) Tricuspid regurgitant volume quantification. TR regurgitant volume is calculated as the difference between RV stroke volume and net pulmonary forward flow, with the corresponding regurgitant fraction. (**E**) Effective RVEF quantification. Effective RVEF is calculated as net pulmonary forward flow divided by RV end-diastolic

volume, providing a measure of effective forward RV performance that accounts for TR. Abbreviations: CMR, cardiovascular magnetic resonance; EDV, end-diastolic volume; ESV, end-systolic volume; RV, right ventricle; RVEDV, right ventricular end-diastolic volume; RVEF, right ventricular ejection fraction; RVESV, right ventricular end-systolic volume; RVSV, right ventricular stroke volume; TR, tricuspid regurgitation.

Additional support for eRVEF comes from the TRILUMINATE study, in which 69 patients with symptomatic severe TR were randomized to transcatheter edge-to-edge repair or medical therapy and underwent serial CMR and 4D-CT. When right heart size and function were compared across tertiles of TR regurgitant volume, conventional RVEF was comparable across increasing TR severity, whereas eRVEF declined progressively as TR severity rose, suggesting that eRVEF captures the hemodynamic burden of TR in a manner that conventional RVEF does not. Importantly, TR reduction after treatment produced a rise in eRVEF, whereas conventional RVEF declined [11], a pattern consistent with restoration of forward flow after elimination of regurgitant volume rather than an acute change in intrinsic contractility.

2.2. RV/LV Volume Ratio

The RV/LV volume ratio (RV/LVvol) is a CMR-derived index that expresses RV end-diastolic volume (RVEDV) relative to LV end-diastolic volume, rather than evaluating RV size or function in isolation. It captures disproportionate RV dilation (i.e., whether the RV has enlarged out of proportion to the LV) and has been shown to help increase the rate at which RV enlargement is detected in PAH [12].

Disproportionate RV enlargement does not occur in isolation. Because the RV and LV share the interventricular septum and a common pericardial space, RV enlargement mechanically encroaches on LV filling via septal shift. This ventricular interdependence is the physiologic rationale behind the RV/LVvol index, as it captures the relational component of remodeling, how much the RV has outgrown the LV, rather than simply how large the RV has become in absolute terms. This distinction matters because absolute RV dilation and relative RV-to-LV disproportion do not always track together, and a substantial proportion of patients with normal indexed RV volumes exhibit an abnormal ratio [12,13]. Because the ratio is a quotient, however, it is not specific to right-sided remodeling. An elevated ratio may reflect RV enlargement, a reduction in LV end-diastolic volume (e.g., from LV underfilling, hypovolemia, or a small or hypertrophied LV cavity), or both, whereas coexisting LV dilation, as in left-sided cardiomyopathy or valvular disease, may lower the ratio and mask substantial RV enlargement. The RV/LVvol ratio should therefore be interpreted alongside indexed RV and LV volumes and LV function rather than in isolation.

A recent retrospective single-center study evaluated the RV/LVvol ratio (dichotomized as normal < 1.27 vs. abnormal ≥ 1.27, a prespecified threshold based on previously established RV/LVvol severity partitions) in 949 patients with at least moderate TR undergoing CMR [13]. Notably, among 528 patients with an otherwise normal RV end-diastolic volume index, 178 (33.7%) still had an abnormal RV/LVvol ratio, indicating that the ratio identifies adverse remodeling in a substantial subset of patients whose RV size alone would be read as unremarkable. Over a mean follow-up of 4.8 ± 4.5 years, an abnormal RV/LVvol ratio was independently associated with increased all-cause mortality (adjusted HR 1.47, 95% confidence interval [CI] 1.01–2.14), with risk rising further in the most severe strata (adjusted HR 2.20, 95% CI 1.31–4.76). The ratio also provided significant incremental prognostic value beyond conventional indices including RVEF and RV end-diastolic volume index. Notably, patients with an elevated ratio had higher LVEF and lower myocardial scar burden than those with a normal ratio, despite their higher mortality, suggesting that the ratio's

prognostic signal reflects right-sided remodeling and RV-LV disproportion specifically, rather than simply signifying co-existing LV dysfunction [13].

Beyond TR, the RV/LVvol ratio has also demonstrated prognostic utility in PH, a setting in which the mechanism driving RV-LV disproportion differs from that in TR. Whereas volume overload in functional TR primarily distends the RV directly, PH imposes chronic pressure overload that both remodels the RV and constrains the LV through leftward septal shift and reduced LV preload from impaired forward flow across the pulmonary vasculature [14,15]. As shown in a clinical and experimental model, with sustained underfilling, the LV may undergo atrophic remodeling with measurable reduction in LV mass and end-diastolic volume, a process shown to be reversible following relief of RV pressure overload [16]. The RV/LVvol ratio is therefore positioned to capture a bidirectional process specific to PH: the ratio rises from both numerator and denominator, reflecting simultaneous RV enlargement and relative LV underfilling driven by the same underlying afterload elevation [17].

A prospective study applied the same RV/LVvol ratio threshold ($\geq$1.27) to 135 patients with PH (defined by pulmonary arterial systolic pressure > 35 mmHg on echocardiography or mean pulmonary artery pressure [mPAP] > 20 mmHg on invasive catheterization) undergoing CMR [17]. An abnormal ratio was present in 41.5% of patients. Over a mean follow-up of 1.9 years, patients with an abnormal RV/LVvol ratio had higher rates of the composite primary outcome (all-cause mortality or heart failure hospitalization) than those with a normal ratio (64.3% vs. 50.0%, $p = 0.02$). After multivariable adjustment for age and CMR indices, an abnormal ratio remained independently associated with the primary outcome (adjusted HR 1.81, 95% CI 1.06–2.97, $p = 0.003$), and it added significant incremental prognostic value beyond age and traditional RV indices (global chi-square increasing from 6.7 to 17.4, $p = 0.006$). Limitations of this study include its modest size and a PH definition that combined echocardiographic and invasive criteria, yielding a heterogeneous population that may include patients without invasively confirmed PH.

Together with the TR data above, these findings suggest that the RV/LVvol ratio provides prognostic information in both volume- and pressure-overload states [13,17]. However, both cohorts were studied by the same group using the same threshold, and because the ratio rises through different mechanisms in TR and PH, whether a single cutoff is optimal across disease settings has not been established and requires validation in independent, disease-specific cohorts.

2.3. Right Atrioventricular Coupling Index (RACI)

The right atrioventricular coupling index (RACI) is a CMR-derived index defined as the ratio of right atrial (RA) to RV end-diastolic volume [18]. Unlike effective RVEF, the RV/LVvol ratio, or hepatic ECV, each of which characterizes either the RV in isolation or a downstream systemic consequence of RV dysfunction, RACI is designed to integrate RA and RV remodeling into a single metric that captures the volumetric relationship between the two chambers rather than either chamber alone.

Underlying RACI is the RA's active modulation of RV filling via its reservoir, conduit, and contractile functions. In early TR, the RA dilates preferentially to accommodate regurgitant volume while maintaining low filling pressures, a compensatory adaptation that keeps the RA-RV hemodynamic interplay in a balanced state. As TR progresses, however, the thinner-walled RA, plausibly more susceptible than the RV to stretch-mediated neurohormonal signaling, dilates disproportionately to RV enlargement, such that the RA-to-RV volume ratio rises and reflects a form of atrioventricular uncoupling. The transition from adaptive RA dilation to a decompensated, uncoupled state may reflect exhaustion of the RA's compensatory reserve and impaired RV filling, and may precede overt RV dysfunc-

tion [18]. Because RACI depends on RA volume, it may also be influenced by factors that enlarge the RA independently of RV remodeling, most notably atrial fibrillation, which is common in functional TR and can also complicate volumetric quantification.

A study of 633 patients with at least moderate functional TR undergoing CMR evaluated RACI using a Youden-index-derived cutoff (normal < 0.62 vs. high ≥ 0.62) [18]. Notably, patients with high RACI had substantially larger RA volumes and smaller RV volumes than those with normal RACI, but with no significant difference in RVEF, underscoring that RACI captures remodeling not reflected by RV function alone. Over a median follow-up of 2.9 years, high RACI was associated with an increased risk for all-cause mortality (25% vs. 15%, HR 2.06, 95% CI 1.47–2.90). This association persisted after adjustment for age, right- and left-heart size and function, and clinical markers of right-sided congestion (adjusted HR 1.16 per 0.10 increase in RACI, 95% CI 1.03–1.32). RACI also provided significant incremental prognostic utility beyond conventional right heart indices, including RA and RV volumes, RVEF, and TR severity, improving model performance (chi-square increasing from 28.5 to 37.6, $p = 0.003$). Notably, when RACI was entered into the model first, RA and RV volumes no longer added significant prognostic value, suggesting that RACI consolidates the prognostic information of both chambers into a single metric that reflects their hemodynamic interplay [18]. Of note, RACI has been evaluated in a single-center cohort, and the $\geq$0.62 cutoff was derived by Youden-index (receiver-operating-characteristic [ROC]) analysis within the same cohort in which its prognostic value was tested, which may overestimate its discriminatory performance. The cutoff has not yet been validated in an independent population or in other right-heart diseases such as PH.

2.4. Nonischemic Septal Fibrosis

Nonischemic septal fibrosis (NIsF) is a CMR late gadolinium enhancement (LGE)-based marker of myocardial tissue injury, defined as hyperenhancement in the midmyocardial or epicardial regions of the interventricular septum, a pattern distinct from the subendocardial or transmural enhancement characteristic of ischemic scar. Unlike effective RVEF, the RV/LVvol ratio, or RACI, which are all volumetric or functional indices, NIsF represents a direct tissue-characterization marker, as it captures structural myocardial injury rather than chamber size or ejection performance [19].

Mechanistically, NIsF is grounded in ventricular interdependence. The interventricular septum is shared by both ventricles and directly transmits mechanical stress between them, such that chronic RV volume overload, as occurs in progressive functional TR, is thought to elevate septal wall stress and, over time, promote myocardial injury and interstitial fibrosis. NIsF may therefore represent a structural signature of the same interventricular mechanical stress that produces the septal geometric changes described earlier in this review, marking a stage of myocardial injury that accompanies chamber dilation and dysfunction [19].

A study of 663 patients with advanced ($\geq$moderate) functional TR undergoing CMR found NIsF present in 29.4% of patients [19]. NIsF was strongly associated with adverse chamber remodeling, including larger LV and RV volumes, reduced systolic function, and greater TR severity (all $p < 0.001$). Notably, TR regurgitant fraction increased in a stepwise fashion with the extent of NIsF (34.9% with no NIsF, 38.1% with one affected segment, 40.8% with two segments, $p < 0.001$). Over a mean follow-up of 4.3 years, NIsF was independently associated with all-cause mortality (HR 1.79, 95% CI 1.26–2.56, $p = 0.001$), even after adjusting for conventional risk markers including age, TR severity, and RV dysfunction and dilation, indicating that septal tissue injury provides prognostic information beyond what chamber size and function alone capture [19]. Limitations of the current evidence include derivation from a single-center cohort, the use of binary presence and segmental extent rather than a validated quantitative threshold, and an observational design that cannot

exclude that nonischemic septal LGE reflects coexisting myocardial disease rather than TR-related septal stress.

2.5. Hepatic Extracellular Volume Fraction

Hepatic extracellular volume fraction (ECV) is a CMR T1-mapping-derived, indirect marker of hepatic extracellular space expansion, which may reflect edema, venous congestion, and/or fibrosis [20]. The extracellular volume fraction is obtained by comparing pre- to post-contrast T1 changes in the liver and blood after correcting for hematocrit (i.e., ECV = (1 − hematocrit) × (ΔR1[liver]/ΔR1[blood])) [21]. A higher hepatic ECV reflects a greater proportion of extracellular space within the liver, consistent with the sinusoidal dilation and interstitial expansion seen in chronic venous congestion [22].

The physiologic rationale is rooted in the systemic consequences of chronic TR. Sustained TR transmits elevated right-sided filling pressures backward into the systemic venous system, producing chronic hepatic venous congestion. Over time, this congestion drives expansion of the hepatic extracellular space through sinusoidal dilation and fibrosis [22]. Because hepatic ECV directly quantifies this extracellular space expansion, it functions as a marker of venous congestion and hepatic remodeling, thus capturing a downstream systemic consequence of RV and tricuspid dysfunction that conventional imaging indices do not directly measure [23]. However, hepatic ECV is not specific to right-heart dysfunction and should not be regarded as a cardiac biomarker per se. Expansion of the hepatic extracellular space also occurs in intrinsic liver disease, including hepatic fibrosis and cirrhosis of other etiologies [20], and hepatic T1 values may be further influenced by inflammation, steatosis, and iron deposition. Elevated hepatic ECV may also reflect venous congestion from causes other than RV remodeling, such as constrictive physiology or left-sided heart failure with secondary PH. Accurate calculation additionally requires a contemporaneous hematocrit measurement. Hepatic ECV should therefore be interpreted in the context of coexisting liver disease and the overall clinical picture [22].

In a recent single-center study, Villar-Calle et al. evaluated hepatic ECV in 234 consecutive patients with at least moderate TR undergoing CMR with hepatic T1 mapping [23]. Mean hepatic ECV was 37.7 ± 9.0%, and patients were stratified into tertiles (cutoffs at 32.5% and 41.3%). Higher hepatic ECV tertiles were associated with worse biventricular function and greater TR severity. Notably, RVEF decreased across tertiles, while the RVEDV index (RVEDVi) increased. Additionally, hepatic ECV provided prognostic information for all-cause mortality beyond conventional risk markers, supporting its role as a marker of systemic congestion with independent prognostic value in TR [23]. Of note, these tertile cutoffs were data-driven and were not intended as clinical decision thresholds.

Margonato et al. reported similar findings in a retrospective cohort of 489 patients referred for CMR in whom TR was quantified by tricuspid regurgitant fraction alongside mapping for hepatic ECV [24]. In a subset of 371 patients with liver mapping data, a hepatic ECV threshold of 32% or greater was associated with clinical manifestations of right-sided heart failure and with long-term adverse outcomes, and it demonstrated incremental prognostic value in survival analysis. Notably, this externally derived threshold of 32% closely approximates the lower tertile cutoff of 32.5% identified in the single-center cohort led by Villar-Calle et al. [23], providing further support for a hepatic ECV value in the low thirties as a potentially meaningful inflection point for congestive hepatic remodeling in TR, although neither value has been prospectively validated as a clinical threshold.

2.6. RV–Pulmonary Artery Coupling in PH: CMR-Derived Surrogates

RV-PA coupling reflects the ability of the RV to adapt its contractility to pulmonary vascular afterload. The invasive reference standard is the ratio of end-systolic elastance to

arterial elastance (Ees/Ea), representing RV contractility and afterload, respectively. Optimal coupling occurs at an Ees/Ea ratio of approximately 1.5–2.0, whereas values around 0.7 have been associated with RV-PA uncoupling and the transition toward maladaptive RV remodeling. However, invasive assessment of RV–PA coupling is technically demanding, time-consuming, expensive, and not widely available, limiting its routine clinical application. Consequently, several noninvasive surrogates have been proposed, predominantly based on echocardiography (e.g., TAPSE, RV fractional area change [RVFAC], RV free-wall longitudinal strain [RVFWLS], or RV global longitudinal strain [RVGLS], each indexed to pulmonary artery systolic pressure [PASP]) [2]. More recently, CMR-derived parameters, the SV/ESV ratio and RV strain, have emerged as potential noninvasive surrogates of RV–PA coupling (with RV strain discussed in a subsequent section).

Tian et al. evaluated CMR-derived SV/ESV in 120 patients with precapillary PH at intermediate risk (76 intermediate-low and 44 intermediate-high). SV/ESV was significantly lower in intermediate-high-risk patients (0.41 vs. 0.56, $p < 0.001$) and independently discriminated intermediate-high risk. A ROC-derived cutoff of <0.51 yielded an area under the curve (AUC) of 0.76 (58% sensitivity, 82% specificity). Over a median follow-up of 62 months, 28% experienced death or heart-failure hospitalization, with SV/ESV < 0.51 associated with significantly worse outcomes ($p = 0.001$). Adding SV/ESV to the European Society of Cardiology/European Respiratory Society (ESC/ERS) four-strata model improved the C-index from 0.60 to 0.74 ($p = 0.008$) [25]. These findings derive from a single-center cohort restricted to intermediate-risk patients, and the cutoff, which had modest sensitivity, was derived within the same cohort and has not been externally validated.

2.7. CMR RV Strain

CMR is considered the gold standard for the quantification of RV volumes and ejection fraction. However, other indices of myocardial deformation may be of interest and provide additional information regarding RV performance. RV strain analysis by feature tracking (FT) can be applied in routinely acquired cine images and has demonstrated RV dysfunction in congenital heart disease and arrhythmogenic RV dysplasia [26,27].

In a study by de Siqueira et al. including 116 patients referred for CMR evaluation of PH, RV strain analysis by FT was feasible in 95% of patients and reproducible, identified subclinical dysfunction and provided independent prognostic information. Peak global circumferential strain rate (GCSR) was significantly reduced in patients with PH despite preserved RVEF compared with healthy controls (−0.92 [−1.0 to −0.7] vs. −1.12 [−1.3 to −0.9] s^{-1}; $p < 0.001$). Global longitudinal strain (GLS) (HR 1.06; $p = 0.026$), GLS rate (GLSR) (HR 2.52; $p = 0.04$), and GCSR (HR 4.50; $p = 0.01$) were independently associated with the composite endpoint of death, lung transplantation, or New York Heart Association (NYHA) functional class deterioration. A GCSR cutoff > −0.8 s^{-1} remained an independent predictor of adverse outcomes after multivariable adjustment [28].

In a prospective study of 38 patients with PH, CMR-derived long-axis RV strain was significantly associated with invasive measures of RV–pulmonary artery coupling (Ees/Ea; $\rho = 0.579$, $p < 0.001$), afterload (Ea; $p = 0.008$), and RV relaxation (Tau; $p < 0.001$), while showing a nonlinear association with RV diastolic stiffness (Eed). RV strain was not directly associated with intrinsic RV contractility (Ees). Long-axis RV longitudinal strain identified impaired RV–pulmonary artery coupling with an AUC of 0.781 using a cutoff of −15.3% [29].

Beyond PH, CMR-derived RV strain has also emerged as a marker of RV dysfunction in patients with TR. In a multicenter study including 544 patients with severe functional TR, Romano et al. demonstrated that CMR FT-derived RV free wall longitudinal strain (RVFWLS) was an independent predictor of all-cause mortality during a median follow-up of 6 years. RVFWLS ≥ −16%, corresponding to the cohort median, was associated with a

significantly higher risk of all-cause mortality after adjustment for clinical and risk factors (HR 1.14 per 1% decrease; $p < 0.001$) [30]. Across these studies, cutoffs were derived by different approaches: the GCSR cutoff was identified in a single-center cohort, the long-axis strain cutoff was ROC-derived against an invasive coupling surrogate in 38 patients rather than against clinical outcomes, and the RVFWLS threshold represents a median split. Because strain values are also vendor- and software-dependent (Section 3.4), none of these cutoffs can yet be considered transferable or externally validated.

2.8. RA Functional Assessment: Strain

RA function can be divided into three phases during the cardiac cycle: reservoir (collecting blood from veins during ventricular systole), conduit (passive passage of blood to RV during early diastole and diastasis), and booster pump (RA active contraction during late diastole). The RA function is essential in regulating RV filling and maintaining cardiac output.

RA strain can be derived from standard four-chamber cine CMR images using FT analysis. Tracking of the RA endocardial contour throughout the cardiac cycle generates strain curves that characterize the three phases of atrial function. Reservoir strain (εs) reflects total RA deformation during atrial filling, conduit strain (εe) represents passive atrial deformation during early ventricular diastole, and booster-pump strain (εa) reflects active atrial contraction. Volumetric assessment (by the area-length method) can be performed by measuring maximal, pre-atrial contraction, and minimal RA volumes, from which total, passive, and active RA emptying fractions can be derived [31].

Yang et al. evaluated 96 patients with precapillary PH, including 36 patients without RV systolic dysfunction, defined as a CMR-derived RVEF ≥ 45%. In this subgroup, RA reservoir (εs) and conduit strain (εe) were significantly impaired compared with healthy controls, despite the absence of significant morphological changes in either the RA or RV. RA conduit strain showed the highest discriminatory ability compared with healthy controls (AUC 0.96; 95% CI 0.91–1.00; sensitivity 92%; specificity 100%; cutoff 26%). In contrast, the 60 patients with RV systolic dysfunction showed larger RA volumes and further impairment in reservoir and conduit function, as well as reduced booster-pump strain (εa). During a median follow-up of 97 months, 45% of patients died. RA reservoir strain was an independent predictor of all-cause mortality (HR = 0.963, $p = 0.014$). Patients with εs ≤ 27% had significantly worse survival on Kaplan–Meier analysis (log-rank $p = 0.002$) [31].

More recently, in a prospective study of 348 patients with PH, Guo et al. evaluated the prognostic value of RA strain over a median follow-up of 41.5 months. RA reservoir strain independently predicted all-cause mortality (adjusted HR 0.950 per 1% increase; 95% CI 0.922–0.979; $p < 0.001$), and values ≤ 16.1% were associated with a 5.6-fold higher risk of death. Data-derived thresholds of 16.1% and 36.8% identified high, intermediate, and low risk groups with 1-year mortality rates of 24.0%, 5.5%, and 0%, respectively. Among CMR-derived metrics, RA reservoir strain showed the highest prognostic discrimination (overall C-index 0.73; 1-year C-index 0.79), and its addition to the REVEAL Lite 2 score increased the 1-year C index from 0.79 to 0.88 ($p = 0.03$). In the subgroup of 182 PAH patients without shunts, RA reservoir strain remained the best performing CMR metric (1-year C-index 0.77) [32].

Beyond pressure overload conditions such as PH, assessment of RA function may also provide clinically relevant information in patients with TR, where chronic volume overload leads to progressive RA and RV remodeling.

In a cohort of 47 patients with predominantly secondary TR (83%), Kim et al. evaluated the relationship between CMR-derived right heart parameters and invasively measured right atrial pressure (RAP). The mean invasively measured RAP was 10 mmHg. RA longitudinal

strain showed an inverse correlation with mean RAP ($r = -0.59$, $p < 0.001$), whereas RVEF and RV longitudinal strain were not significantly associated with RAP. In multivariable analysis, RA longitudinal strain and RVEDVi remained independently associated with mean RAP. RA longitudinal strain demonstrated good discrimi.

Nation for elevated RAP (>10 mmHg), with an AUC of 0.82, compared with 0.78 for RVEDVi [33]. Collectively, the RA strain literature is limited by small or single-center cohorts, including the retrospective single-center study by Yang et al. [31], and by thresholds derived within each cohort. Proposed reservoir strain cutoffs for mortality differ substantially between studies (≤27% [31] vs. ≤16.1% [32]), likely reflecting differences in populations, disease severity, and post-processing, and the study by Kim et al. used invasive RAP as a hemodynamic surrogate rather than clinical outcomes [33].

2.9. Myocardial T1/ECV Mapping: Diffuse Fibrosis Beyond Focal LGE

Beyond the assessment of extracardiac remodeling with hepatic ECV, myocardial T1 mapping may provide complementary information on diffuse RV myocardial remodeling. However, quantitative tissue characterization of the RV is challenging because of its thin wall and complex structure. Current T1 mapping methods, such as modified Look-Locker inversion recovery imaging (MOLLI) have insufficient spatial resolution for RV fibrosis imaging.

Asano et al. demonstrated the prognostic value of RV free-wall native T1 mapping using end-systolic MOLLI in 30 patients with PAH. RV native T1 was significantly higher than in controls (1384 ± 74 vs. 1217 ± 57 ms; $p < 0.001$) and independently predicted death or hospitalization (HR 1.02; $p = 0.002$), although limited by the small sample size and retrospective design [34].

Using high-resolution accelerated and navigator-gated Look-Locker imaging for cardiac T1 estimation (ANGIE), Mehta et al. demonstrated increased RV extracellular volume in patients with PH. In a cohort of 32 subjects (12 with PH, 10 with heart failure with reduced ejection fraction [HFrEF] without PH, and 10 healthy controls), RV ECV was higher in patients with PH than in healthy controls (34.1% vs. 26.8%, $p < 0.0001$). RV ECV was also associated with increasing RVEDVi and decreasing RVEF, while PH remained independently associated with increased RV ECV after adjustment for RV dilatation and dysfunction [35]. This study was small and did not evaluate clinical outcomes, and thresholds for RV native T1 and ECV have not been established.

2.10. CMR Markers of Treatment Response and Reverse Remodeling

In evaluating CMR markers of treatment response, three categories should be distinguished: baseline markers associated with subsequent response, markers that quantify changes after treatment, and markers prospectively validated to predict treatment benefit or improve treatment selection. To date, no CMR marker in either PH or TR has met the last criterion.

In patients with PAH, Goh et al. evaluated whether baseline CMR-derived RV remodeling patterns could predict subsequent reverse remodeling after treatment. RV phenotypes were defined according to RV end-systolic volume index and ventricular mass index as: (1) low-volume, low-mass; (2) low-volume, high-mass; (3) high-volume, high-mass; and (4) high-volume, low mass. The high-volume low-mass phenotype was associated with the worst prognosis, with significantly higher all-cause mortality compared with each of the other remodeling phenotypes over a median follow-up of 4.85 years. Among patients with follow-up CMR assessment, reverse remodeling toward the adaptive low-volume low-mass phenotype occurred in 59.1% of patients with baseline low-volume high-mass and 30.0% of those with high-volume high-mass phenotypes, compared with only 17.4% of patients with

a high-volume low-mass phenotype, suggesting that the latter represents a maladaptive remodeling pattern with limited potential for reverse remodeling following treatment [36].

Additional studies have investigated the role of CMR-derived RV volumes in assessing treatment response. Celant et al. identified baseline CMR RVEDV as an independent predictor of achieving or maintaining RVEF ≥ 45% after treatment in 127 patients with PAH. This threshold was reached by 59% of patients and associated with stable RV function during long-term follow-up and improved survival [37]. In a study that included 63 patients with PAH, Rischard et al. identified treatment-associated reduction in RVEDV of ≥15 mL at 11 months as the optimal CMR marker of RV functional recovery based on its ability to discriminate preserved exercise capacity (VO_2peak > 15 mL/kg/min; AUC 0.87; $p = 0.0001$). This threshold was achieved by 35% of patients and associated with a lower incidence of clinical worsening [38]. These PH studies were observational, and their proposed markers, including the ROC-derived ≥ 15 mL RVEDV reduction, have not been prospectively validated to guide therapy.

In contrast to PH, validated baseline CMR predictors of RV reverse remodeling after transcatheter tricuspid interventions remain lacking. Current CMR evidence supports the quantification of RV reverse remodeling rather than prediction of treatment response. In the TRILUMINATE Pivotal imaging substudy, CMR demonstrated a significant reduction in RVEDV, RA end-diastolic volume (RAEDV), and tricuspid annular area at 30 days after tricuspid transcatheter edge-to-edge repair (T-TEER), with the magnitude of TR reduction strongly associated with the reduction in RVEDV ($r = 0.90$; $p < 0.0001$). RVEF decreased with greater TR reduction (up to −8 percentage points in patients with large reduction), whereas effective RVEF increased (up to +12 percentage points) [11]. These data describe post-treatment remodeling and do not establish that baseline CMR indices predict which patients will benefit from intervention.

2.11. 4D-Flow CMR and Pulmonary Artery Hemodynamics

In PH, chronic increases in pulmonary artery pressure and pulmonary vascular resistance induce remodeling of the central pulmonary arteries, characterized by progressive dilatation and stiffening. 4D-flow CMR enables comprehensive assessment through visualization of 3D blood flow (flow pattern, vortical flow), conventional blood flow parameters typically obtained by 2D phase-contrast CMR and advanced hemodynamic parameters, such as wall shear stress (WSS), vorticity, helicity and energy loss [39].

While normal pulmonary artery flow is predominantly laminar, increasing mPAP is associated with the development and greater persistence of vortical flow [39]. In a study that included 145 patients with suspected PH, Reiter et al. demonstrated an association between vortex duration (tVortex), expressed as the percentage of the cardiac cycle during which a vortex was present, and invasively measured mPAP ($R^2 = 0.95$). A tVortex cutoff of 14.3% identified PH with an AUC of 0.99, 97% sensitivity, and 96% specificity [40]. Notably, this cutoff was derived and evaluated in the same cohort without a separate validation group, so its diagnostic performance may be overestimated, and it addresses diagnosis rather than prognosis.

Wall shear stress (WSS), reflecting the frictional force exerted by blood flow on the vascular wall, represents another 4D-flow-derived marker related to pulmonary vascular remodeling. Kim et al., using 4D-flow CMR and right heart catheterization in 28 patients with PH, demonstrated lower mean main pulmonary artery (MPA) WSS in PAH compared with PH-HFpEF (0.29 ± 0.09 vs. 0.36 ± 0.06 Pa; $p = 0.035$), with mean WSS inversely correlated with invasively measured pulmonary vascular resistance (PVR) ($r = -0.63$; $p = 0.002$) [41].

Beyond hemodynamic characterization, 4D-flow-derived parameters may also reflect treatment-associated reverse remodeling. In this context, helicity describes the relationship between flow strength and the amount of local rotation in flow. In 20 patients with chronic thromboembolic pulmonary hypertension (CTEPH) undergoing pulmonary endarterectomy, Dong et al. demonstrated that treatment-associated changes in MPA helicity were associated with RV reverse remodeling, with reductions in RV end-systolic volume (RVESV) significantly related to changes in the fraction of positive helicity ($r = 0.75$, $p = 0.003$) and helical flow index ($r = -0.72$, $p = 0.005$) [42]. Overall, 4D-flow studies in PH remain small, and none of these parameters has an established prognostic threshold.

Representative examples and quantitative assessment of the CMR-derived markers of adverse right-heart remodeling discussed in this review are summarized in Figure 2.

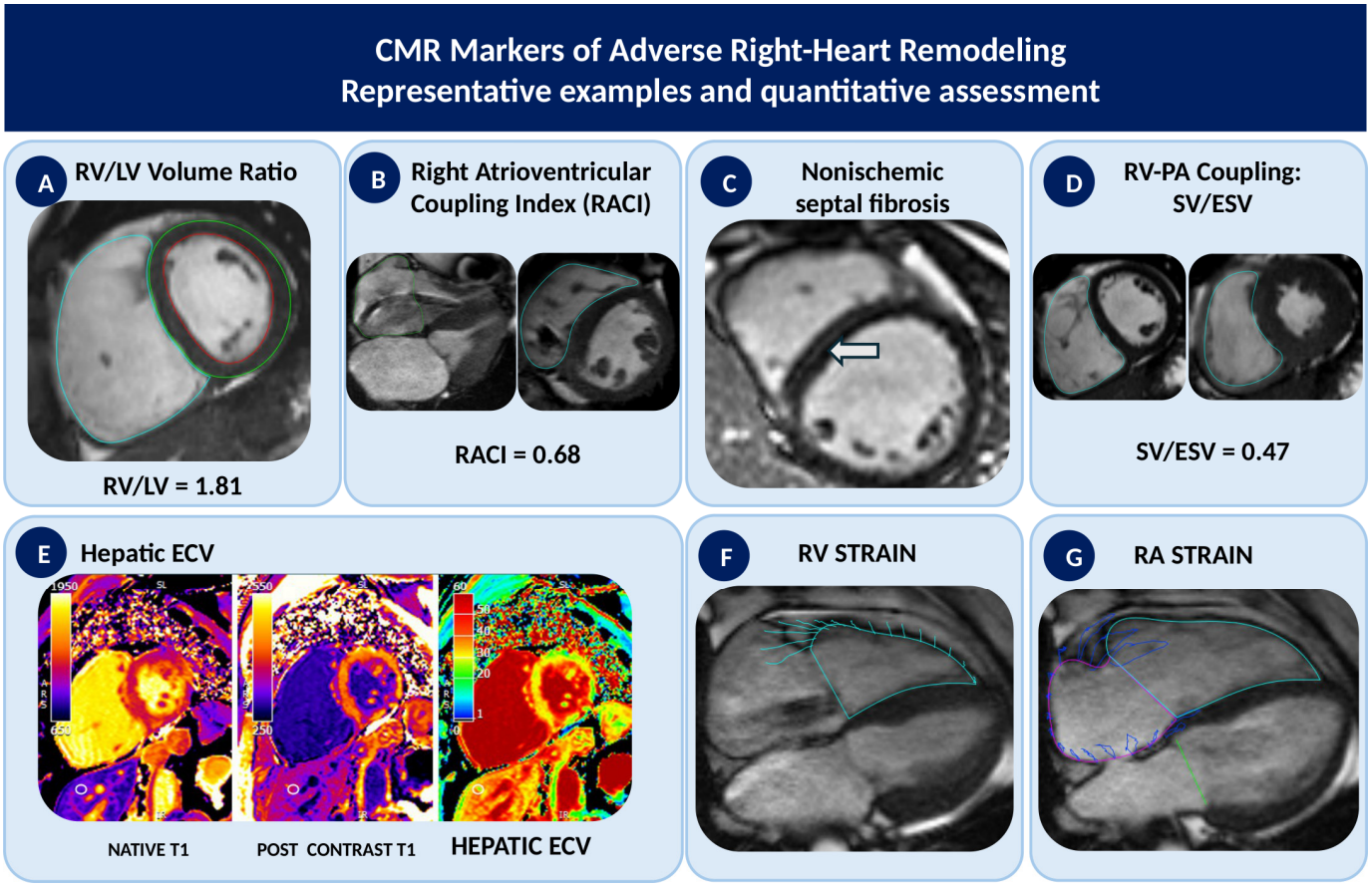


Figure 2. CMR markers of adverse right-heart remodeling: representative examples and quantitative assessment. (**A**) RV/LV volume ratio. Representative short-axis cine CMR demonstrating RV and LV volumetric assessment. In this example, RVEDV was 245 mL and LVEDV was 135 mL, yielding an RV/LV volume ratio of 1.81. (**B**) RACI. Representative CMR images demonstrating RA and RV volumetric assessment. In this example, RA end-diastolic volume was 91 mL and RV end-diastolic volume was 133 mL, yielding a RACI of 0.68. (**C**) Nonischemic septal fibrosis. Representative LGE CMR image demonstrating mid-wall septal fibrosis (arrow), a nonischemic pattern associated with adverse right-heart remodeling. (**D**) RV–PA coupling. Representative cine CMR images demonstrating RV volumetric assessment. SV can be derived as the difference between RVEDV and RVESV, and RV–PA coupling is estimated as the SV/ESV ratio. In this example, RVEDV was 220 mL and RVESV 150 mL, yielding an SV of 70 mL and an SV/ESV ratio of 0.47. (**E**) Hepatic ECV. Representative native T1, post-contrast T1, and derived hepatic ECV maps. ROIs are placed within the liver parenchyma on native and post-contrast T1 maps to obtain hepatic T1 values. In this example, native T1 was 866 ms, post-contrast T1 was 331 ms, and hepatic ECV was 41%. (**F**) Right ventricular strain. Representative

feature-tracking CMR demonstrating endocardial contouring of the RV in the four-chamber view for assessment of longitudinal myocardial deformation. (**G**) Right atrial strain. Representative feature-tracking CMR demonstrating RA endocardial contouring in the four-chamber view for assessment of atrial longitudinal strain. Abbreviations: CMR, cardiovascular magnetic resonance; ECV, extracellular volume; LGE, late gadolinium enhancement; LV, left ventricle; PA, pulmonary artery; RA, right atrium; RACI, right atrioventricular coupling index; ROI, region of interest; RV, right ventricle; RVEDV, right ventricular end-diastolic volume; RVESV, right ventricular end-systolic volume; SV, stroke volume.

3. Discussion

Collectively, these CMR indices (effective RVEF, hepatic ECV, the RV/LVvol ratio, RACI, and nonischemic septal fibrosis) offer complementary, mechanistically distinct windows into RV remodeling, from effective forward performance to systemic congestion, chamber disproportion, atrioventricular hemodynamic interplay, and myocardial tissue injury. However, none of these indices is specific to a single pathophysiologic process, and each should be interpreted in light of its potential cardiac and noncardiac confounders, as discussed in Sections 2.1–2.5.

3.1. Clinical Relevance

The clinical relevance of this expanded toolkit is amplified by the rapid growth of transcatheter tricuspid valve intervention (TTVI). As transcatheter edge-to-edge repair and transcatheter valve replacement have moved from investigational procedures to standard treatment options for severe TR, the central clinical question has shifted from whether patients can be treated to when they should be treated [43]. Observational evidence suggests that the timing of intervention materially affects outcomes. Once RV remodeling becomes sufficiently advanced, reverse remodeling after TR reduction becomes less complete, and mortality and heart failure hospitalization risk after TTVI remain elevated even when the procedure itself is technically successful [43,44]. This provides a rationale for evaluating the indices reviewed here in this context. Several of these indices capture adverse RV remodeling either at a stage when conventional volumetric and functional metrics remain normal or through a distinct mechanistic lens, and could, in principle, help identify high-risk patients before remodeling reaches a less reversible stage, potentially shifting the point of referral from the appearance of symptoms or overt RV dysfunction toward earlier identification of patients whose RV retains greater capacity for reverse remodeling.

It is important, however, to distinguish prognostic association from demonstrated clinical utility. The evidence summarized in this review consists largely of observational studies showing that these indices are independently associated with outcomes or improve the discrimination of risk models. Such data establish that an index carries prognostic information, but not that its use changes management or improves patient outcomes. In particular, no study to date has shown that selecting or timing tricuspid intervention on the basis of any of these indices improves outcomes, and evidence that they predict which patients will benefit from TTVI, as opposed to which patients are at higher risk regardless of treatment, remains limited. Current CMR data in TTVI largely describe remodeling after treatment rather than baseline predictors of treatment response (Section 2.10) [11]. Similarly, in PH, baseline remodeling phenotypes and volumetric changes have been associated with treatment response [36–38], but CMR-guided therapeutic strategies have not been tested against standard care.

Before these indices can be used to guide management, several types of additional evidence are needed: (1) prospective, multicenter validation of standardized acquisition and analysis methods and of prespecified, disease-specific thresholds; (2) demonstration that the indices identify patients who derive differential benefit from intervention, ideally

through analyses of treatment-by-index interaction within randomized trials of TTVI or PH-directed therapy; (3) studies testing whether index-guided referral or treatment timing improves clinical outcomes compared with conventional assessment, including randomized strategy trials; and (4) evaluation of reverse remodeling and outcomes after intervention according to baseline index values. Until such data are available, these indices are best regarded as tools that refine risk stratification and phenotyping and that may inform, but should not yet determine, clinical decision-making.

3.2. Comparison with Conventional CMR, Echocardiographic, and Clinical Risk Measures

Conventional RVEF and indexed RV volumes. Most of the reviewed indices have been evaluated against conventional RVEF and indexed RV volumes, and several provide information that these measures do not capture. Effective RVEF improved mortality prediction when added to conventional RVEF, whereas conventional RVEF added no information to effective RVEF [10], and the two moved in opposite directions after TR reduction [11]. An abnormal RV/LVvol ratio was present in one-third of patients with a normal RVEDVi and added prognostic value beyond RVEF and RVEDVi [13]. Patients with high RACI had similar RVEF to those with normal RACI, and RA and RV volumes no longer added prognostic value once RACI was considered [18]. NIsF and hepatic ECV remained associated with mortality after adjustment for RV size and function [19,23]. Among functional markers, RV circumferential strain rate and RA reservoir and conduit strain were impaired in patients with PH and preserved RVEF [28,31], and RA strain correlated with invasive RAP, whereas RVEF and RV longitudinal strain did not, and discriminated elevated RAP better than RVEDVi [33]. These comparisons, however, were largely performed within the derivation cohorts using nested models, a setting that tends to favor the novel index. Head-to-head comparisons in independent cohorts, together with reclassification and calibration analyses, are needed to confirm that the incremental value is clinically meaningful.

Echocardiography. Echocardiography remains the first-line modality for assessing TR and PH, and several echocardiographic parameters, including TAPSE, RV fractional area change, RV free-wall strain, RA strain, and TAPSE/PASP as a surrogate of RV–PA coupling [2], address physiological domains analogous to the CMR indices reviewed here. Head-to-head comparisons between these CMR indices and comprehensive echocardiographic assessment remain limited, and it is not yet established whether CMR indices add prognostic information beyond a complete echocardiographic evaluation. In practice, CMR is most likely to add value when echocardiographic windows are limited, when RV size and function are difficult to assess because of the RV's complex geometry, or when TR severity or RV function is uncertain or discordant across modalities.

Established clinical risk scores. In PH, two CMR markers have been evaluated against established multiparametric risk tools: adding SV/ESV to the ESC/ERS four-strata model improved the C-index from 0.60 to 0.74 in intermediate-risk patients [25], and adding RA reservoir strain to the REVEAL Lite 2 score increased the 1-year C-index from 0.79 to 0.88 [32]. These findings suggest that CMR can complement guideline-endorsed risk assessment in PH, but both were single-cohort analyses requiring external confirmation. In TR, the incremental value of the reviewed indices over TR-specific clinical risk scores has not, to our knowledge, been systematically evaluated, and integrating CMR indices with such scores represents an important next step.

3.3. Comparative Strength of Evidence and Generalizability of Proposed Thresholds

The indices reviewed here differ substantially in validation status, reproducibility, and readiness for clinical use, and their supporting evidence should not be regarded as equivalent (Tables 1 and 2). Broadly, they can be grouped into three levels of evidence maturity.

Table 1. Novel cardiac magnetic resonance indices of adverse right heart remodeling: mechanistic domain, definition, proposed thresholds, and clinical/prognostic evidence.

Index	Mechanistic Domain	CMR Definition	Clinical Setting	Proposed Threshold	Cohort	Threshold Derivation and Status	Key Clinical/Prognostic Association
Effective RVEF	Effective forward RV performance	Forward stroke volume/RV end-diastolic volume	Functional TR	≤25%	453 (derivation); 316 in 2 external validation cohorts	Derived from mortality data; tested in 2 external TR cohorts; not tested in PH	Independently predictive of all-cause mortality after adjustment for TR severity, RV size, and conventional RVEF; incremental over conventional RVEF [10]. Threshold remained prognostic in both external cohorts (HR 2.66–2.86) [10].
RV/LV volume ratio	Interventricular disproportion (ventricular interdependence)	RV end-diastolic volume/LV end-diastolic volume	Functional TR	≥1.27	949; retrospective, single-center	Prespecified (established severity partitions); not externally validated	Adjusted HR 1.47 (95% CI 1.01–2.14); 2.20 (1.31–4.76) in the most severe strata. Abnormal in 33.7% of patients with normal indexed RVEDV [13].
RV/LV volume ratio	Interventricular disproportion (ventricular interdependence)	RV end-diastolic volume/LV end-diastolic volume	Pulmonary hypertension	≥1.27	135; prospective	Prespecified; same threshold as TR cohort; not externally validated	Adjusted HR 1.81 (95% CI 1.06–2.97) for mortality or HF hospitalization; global χ^2 6.7 → 17.4 ($p = 0.006$) [17].
RACI	Right atrioventricular coupling	RA end-diastolic volume/RV end-diastolic volume	Functional TR	≥0.62 (Youden)	633; single-center	Youden (ROC)-derived in same cohort; not externally validated	HR 2.06 (95% CI 1.47–2.90); adjusted HR 1.16 per 0.10 increase (1.03–1.32); global χ^2 28.5 → 37.6 ($p = 0.003$) [18].
Nonischemic septal fibrosis	Myocardial tissue injury	Midmyocardial or epicardial septal late gadolinium enhancement	Functional TR	Presence (extent by segment)	663; single-center	No numerical threshold (presence/extent)	Present in 29.4%. HR 1.79 (95% CI 1.26–2.56, $p = 0.001$) after adjustment for age, TR severity, and RV dysfunction and dilation [19].
Hepatic ECV	Downstream systemic venous congestion	(1 − Hct) × (ΔR1 liver/ΔR1 blood) on T1 mapping	Functional TR	Tertiles at 32.5% and 41.3%	234; single-center	Data-driven tertiles; not a clinical threshold	Higher tertiles associated with worse biventricular function and greater TR severity; prognostic for all-cause mortality beyond conventional risk markers [23].
Hepatic ECV	Downstream systemic venous congestion	(1 − Hct) × (ΔR1 liver/ΔR1 blood) on T1 mapping	TR (patients referred for CMR)	≥32%	371 with liver mapping (of 489); retrospective	Independently derived; concordant with tertile cutoff above; not prospectively validated	Associated with clinical manifestations of right-sided heart failure and long-term adverse outcomes; incremental prognostic value in survival analysis. Threshold closely approximates the lower tertile cutoff (32.5%) of the independent cohort above [24].

Table 1. *Cont.*

Index	Mechanistic Domain	CMR Definition	Clinical Setting	Proposed Threshold	Cohort	Threshold Derivation and Status	Key Clinical/Prognostic Association
RV-PA coupling: SV/ESV	RV-PA coupling	RV stroke volume/RV end-systolic volume	Precapillary PH	<0.51	120; single-center	ROC-derived in same cohort; not externally validated	Lower in intermediate-high vs. intermediate-low risk (0.41 vs. 0.56); AUC 0.76 for intermediate-high risk; <0.51 associated with death/HF hospitalization and improved ESC/ERS four-strata model discrimination (C-index 0.60 → 0.74) [25].
RV global circumferential strain rate (GCSR)	RV myocardial deformation	FT-derived peak global circumferential strain rate	PH	$>-0.8\ s^{-1}$	116; single-center	Proposed in single cohort; not externally validated	Impaired despite preserved RVEF (-0.92 vs. $-1.12\ s^{-1}$ in controls; $p < 0.001$); independently associated with death, lung transplantation, or NYHA class deterioration (HR 4.50; $p = 0.01$) [28].
RV longitudinal strain	RV myocardial deformation/RV-PA coupling	CMR-derived long axis longitudinal strain	PH	>−15.3%	38; prospective	ROC-derived against invasive Ees/Ea (surrogate); not externally validated	Associated with invasive Ees/Ea ($\rho = 0.579$; $p < 0.001$); identified impaired RV–PA coupling with AUC 0.781 at a cutoff of −15.3% [29].
RV free wall longitudinal strain (RVFWLS)	RV myocardial deformation	FT-derived RV free-wall longitudinal strain	Functional TR	≥−16%	544; multicenter	Cohort median; not externally validated	Independently associated with all-cause mortality over a median 6-year follow-up; RVFWLS ≥ −16% identified higher-risk patients (HR 1.14 per 1% decrease; $p < 0.001$) [30].
RA reservoir strain (εs)	RA functional remodeling	FT-derived total RA deformation during atrial filling	PH	≤16.1%	348; prospective	Data-derived in same cohort; differs from other cohorts (≤27% [31])	Independently predicted all-cause mortality (adjusted HR 0.950 per 1% increase); ≤16.1% associated with 5.6-fold higher mortality risk; improved 1-year REVEAL Lite 2 C-index from 0.79 to 0.88 [32].
RV free-wall native T1	Diffuse RV myocardial remodeling	End-systolic RV free-wall native T1 (MOLLI)	PH	Not established	30; retrospective	Not established	Higher in PAH vs. controls (1384 ± 74 vs. 1217 ± 57 ms; $p < 0.001$); independently associated with death or hospitalization (HR 1.02; $p = 0.002$) [34].
RV ECV	Diffuse RV myocardial fibrosis	High-resolution RV free-wall ECV (ANGIE T1 mapping)	PH	Not established	32 (12 PH); prospective	Not established	Higher in PH vs. healthy controls (34.1% vs. 26.8%; $p < 0.0001$); associated with ↑RVEDVi and ↓RVEF and remained independently associated with PH after adjustment for RV dilation and dysfunction [35].

Table 1. *Cont.*

Index	Mechanistic Domain	CMR Definition	Clinical Setting	Proposed Threshold	Cohort	Threshold Derivation and Status	Key Clinical/Prognostic Association
4D Flow: PA vortex duration (tVortex)	Pulmonary vascular hemodynamics	% of cardiac cycle with vortical MPA flow	PH	>14.3%	145; single-center	Model/ROC-derived in same cohort (diagnostic); not externally validated	Associated with invasive mPAP (R^2 = 0.95); >14.3% identified PH with AUC 0.99, 97% sensitivity, and 96% specificity [40].

All thresholds shown are proposed cutoffs from individual studies; none is an established or validated clinical decision criterion. Thresholds are population- and methodology-dependent (e.g., field strength, vendor, sequence, contouring conventions, and post-processing software) and were derived in the disease settings listed; thresholds derived in functional TR should not be assumed to apply to PH, and vice versa. The validation status of each index is further summarized in Table 2. Abbreviations: ANGIE, accelerated and navigator-gated look-locker imaging for cardiac T1 estimation; AUC, area under the curve; CI, confidence interval; CMR, cardiac magnetic resonance; ECV, extracellular volume fraction; Ees/Ea, end-systolic elastance to arterial elastance ratio; ESC/ERS, European Society of Cardiology/European Respiratory Society; FT, feature tracking; GCSR, global circumferential strain rate; HF, heart failure; HR, hazard ratio; Hct, hematocrit; LV, left ventricular; mPAP, mean pulmonary artery pressure; MPA, main pulmonary artery; NYHA, New York Heart Association; PA, pulmonary artery; PAH, pulmonary arterial hypertension; PH, pulmonary hypertension; RA, right atrial; RACI, right atrioventricular coupling index; ROC, receiver operating characteristic; RV, right ventricular; RVEDV, right ventricular end-diastolic volume; RVEDVi, right ventricular end-diastolic volume index; RVEF, right ventricular ejection fraction; RVFWLS, right ventricular free-wall longitudinal strain; SV/ESV, stroke volume to end-systolic volume ratio; TR, tricuspid regurgitation.

Table 2. Comparative summary of study populations, proposed thresholds, endpoints, and validation status of novel CMR indices of right-heart remodeling.

Index	Clinical Setting	Cohort (*n*; Design)	Proposed Threshold (Derivation)	Primary Endpoint	Independent/External Validation	Evidence Maturity
Effective RVEF [10,11]	Functional TR (≥moderate)	453 (derivation); 316 in 2 independent external validation cohorts	≤25% (derived from all-cause mortality data)	All-cause mortality	Threshold remained prognostic in both external cohorts (HR 2.66–2.86); supportive serial data after T-TEER in TRILUMINATE imaging substudy (n = 69); not evaluated in PH	Most mature evidence (closest to clinical implementation)
RV/LV volume ratio [13]	Functional TR (≥moderate)	949; retrospective, single-center	≥1.27 (prespecified; established severity partitions)	All-cause mortality	Same threshold subsequently applied in PH by the same group; no independent external validation	Most mature evidence (closest to clinical implementation)
RV/LV volume ratio [17]	PH	135; prospective	≥1.27 (prespecified; same threshold as TR cohort)	All-cause mortality or HF hospitalization	As above; optimal disease-specific cutoff not established	Most mature evidence (closest to clinical implementation)
RACI [18]	Functional TR (≥moderate)	633; single-center	≥0.62 (Youden index, same cohort)	All-cause mortality	None to date; not evaluated in PH	Promising; requires external validation
Nonischemic septal fibrosis [19]	Functional TR (≥moderate)	663; single-center	Presence; extent by segment	All-cause mortality	None to date; relies on established LGE visual scoring	Promising; requires external validation

Table 2. *Cont.*

Index	Clinical Setting	Cohort (*n*; Design)	Proposed Threshold (Derivation)	Primary Endpoint	Independent/External Validation	Evidence Maturity
Hepatic ECV [23,24]	TR (≥moderate) [23]; TR referred for CMR [24]	234; single-center [23] 371 with liver mapping; retrospective [24]	Data-driven tertiles at 32.5% and 41.3% [23]; ≥32% [24]	All-cause mortality [23]; all-cause mortality or HF hospitalization [24]	Concordant threshold in an independent cohort; limited reproducibility data; confounded by intrinsic liver disease	Promising; requires external validation
SV/ESV [25]	Precapillary PH, intermediate risk	120; single-center	<0.51 (ROC for intermediate-high risk)	Intermediate-high risk status; death or HF hospitalization	None to date; not evaluated in TR	Promising; requires external validation
RV GCSR [28]	PH	116; single-center	$>-0.8\ s^{-1}$ (proposed in single cohort)	Death, lung transplantation, or NYHA class deterioration	None to date; vendor- and software-dependent	Promising; requires external validation
RV longitudinal strain [29]	PH	38; prospective	>−15.3% (ROC vs. invasive Ees/Ea)	Invasive RV–PA coupling (Ees/Ea); hemodynamic surrogate, not clinical outcome	None to date	Promising; requires external validation
RVFWLS [30]	Severe functional TR	544; multicenter	≥−16% (cohort median)	All-cause mortality	Multicenter cohort; vendor- and software-dependent	Promising; requires external validation
RA reservoir strain [31,32]	Precapillary PH [31]; PH [32]	96; single-center, retrospective [31] 348; prospective [32]	≤27% [31]; ≤16.1% (data-derived) [32]	All-cause mortality	Divergent thresholds across cohorts; not standardized	Promising; requires external validation
RV native T1 [34]	PAH	30; retrospective	Not established	Death or hospitalization	None to date	Exploratory
RV ECV (ANGIE) [35]	PH	32 (12 PH); prospective	Not established	None (diagnostic/mechanistic association)	None to date; sequence not widely available	Exploratory
4D-flow tVortex [40]	Suspected PH	145; single-center	>14.3% (model/ROC-derived, same cohort)	Diagnosis of PH (invasive mPAP)	None to date; diagnostic rather than prognostic	Exploratory

Evidence maturity reflects the authors' synthesis of cohort size, number and independence of supporting cohorts, method of threshold derivation, and available reproducibility data; it is not a formal grading system. Thresholds were derived in the populations shown, are methodology-dependent, and should not be assumed to apply to other disease settings; none is a validated clinical decision criterion. Abbreviations: ANGIE, accelerated and navigator-gated look-locker imaging for cardiac T1 estimation; CMR, cardiac magnetic resonance; ECV, extracellular volume fraction; Ees/Ea, end-systolic elastance to arterial elastance ratio; GCSR, global circumferential strain rate; HF, heart failure; LGE, late gadolinium enhancement; mPAP, mean pulmonary artery pressure; NYHA, New York Heart Association; PA, pulmonary artery; PAH, pulmonary arterial hypertension; PH, pulmonary hypertension; RA, right atrial; RACI, right atrioventricular coupling index; ROC, receiver operating characteristic; RV, right ventricular; RVEF, right ventricular ejection fraction; RVFWLS, right ventricular free-wall longitudinal strain; SV/ESV, stroke volume to end-systolic volume ratio; T-TEER, tricuspid transcatheter edge-to-edge repair; TR, tricuspid regurgitation; tVortex, vortex duration.

Indices with the most mature evidence. Effective RVEF has the most mature evidence base among the novel indices, with a threshold derived from mortality data in 453 patients and subsequently tested in two independent external cohorts (combined $n = 316$), demonstrated incremental value over conventional RVEF [10], and supportive serial data from the TRILUMINATE imaging substudy showing that it tracks changes in TR burden after intervention [11]. The RV/LVvol ratio has been associated with outcomes in two cohorts spanning functional TR ($n = 949$) and PH ($n = 135$) [13,17], building on earlier work showing improved detection of RV enlargement [12], although both outcome studies come from a single group. Both indices rely on volumetric (and, for effective RVEF, phase-contrast) measurements that are widely available and reproducible [45,46]. Even for these indices, however, prospective validation of the proposed thresholds, external validation of the RV/LVvol threshold, and evaluation in disease settings other than those in which they were derived are still needed.

Promising indices requiring external validation. RACI, NIsF, hepatic ECV, SV/ESV, and feature-tracking RV and RA strain have each shown independent or incremental prognostic associations, but their supporting evidence is less mature. RACI and NIsF have each been studied in a single-center cohort [18,19], and the RACI threshold was derived by the Youden index within the same population in which its prognostic value was tested. The SV/ESV threshold derives from a single-center cohort of 120 patients with intermediate-risk precapillary PH [25]. Feature-tracking strain has been studied more broadly, including in a multicenter TR cohort [30], but measurements depend on vendor, software, and deformation metric, and proposed thresholds vary across studies [28–32]. Hepatic ECV occupies an intermediate position: its prognostic association has been reported in two independent cohorts with concordant thresholds near 32% [23,24], but reproducibility data remain limited and its specificity for cardiac congestion is reduced by intrinsic liver disease (Section 2.5).

Exploratory indices. RV native T1 and ECV mapping and 4D-flow-derived hemodynamic parameters remain at an early stage. Available studies are small ($n = 20$–145), frequently retrospective or single-center, and rely on sequences or post-processing that are not widely available, and several report diagnostic or mechanistic associations rather than validated prognostic thresholds [34,35,40–42]. These techniques should currently be regarded as research tools.

Generalizability of proposed thresholds. The thresholds summarized in Tables 1 and 2 were derived in specific populations using different methods (prespecified cutoffs, outcome-based or ROC/Youden-derived cutoffs, median splits, or tertile-based stratification) and different endpoints (all-cause mortality, composite clinical outcomes, or invasive hemodynamic surrogates). Because the physiologic substrate of RV remodeling differs between chronic volume overload and chronic pressure overload, thresholds established in functional TR (e.g., effective RVEF $\leq 25\%$ and RACI ≥ 0.62) should not be assumed to apply to PH or other right-heart diseases, and vice versa. Even where the same threshold has been applied across settings, as with the RV/LVvol ratio ≥ 1.27 in TR and PH [13,17], the optimal cutoff may differ by disease. These values are also methodology-dependent, as they may vary with field strength, vendor, acquisition sequence, contouring conventions, and post-processing software. Cutoffs derived within a single cohort, particularly by ROC or Youden-index optimization, are also likely to overestimate performance when applied to new populations. Accordingly, none of these values should be interpreted as a universal decision threshold; until they are prospectively validated in independent, disease-specific cohorts using standardized methods, they should be regarded as hypothesis-generating risk markers rather than established clinical criteria.

3.4. Reproducibility and Technical Challenges

The volumetric methods underlying effective RVEF, the RV/LVvol ratio, and RACI build on chamber quantification techniques with demonstrated high reproducibility in prior work from groups using this approach [45,46]. LGE-based fibrosis assessment for NIsF relies on established semiquantitative visual scoring methods [47]. Reproducibility data specific to hepatic ECV are comparatively less mature, reflecting its more recent development and lower current uptake outside specialized centers.

Even for volumetric indices, measurement variability can be meaningful. RV and RA contours are sensitive to the selection of the basal short-axis slice, the handling of trabeculations and the tricuspid annulus, and the choice of short-axis versus axial or long-axis acquisitions, and RA volumes differ between area-length and summation-of-discs methods. Because effective RVEF, the RV/LVvol ratio, and RACI are ratios of two measured quantities, errors in either component propagate to the index, and reproducibility data for the composite indices themselves, as opposed to their component volumes, remain limited. Effective RVEF additionally depends on accurate phase-contrast flow quantification, which requires appropriate velocity encoding and correction of background phase offsets.

Feature-tracking strain is particularly sensitive to methodological factors. Absolute strain values differ systematically across post-processing platforms, so values and cutoffs derived with one software package are not directly transferable to another. The thin RV free wall, complex RV geometry, through-plane motion, and limited temporal resolution of routine cine imaging further reduce the reproducibility of RV and RA strain compared with LV strain, and strain-rate parameters are generally less reproducible than peak strain.

Regarding these novel functional CMR markers, technical and methodological limitations currently restrict their broader clinical implementation. RV strain studies in right heart disease include heterogeneous cohorts (n = 38–544) and used different field strengths (1.5–3.0 T), scanner vendors (Siemens Healthineers, Erlangen, Germany; Philips Healthcare, Best, The Netherlands; GE HealthCare, Waukesha, WI, USA), post-processing FT software (TomTec, CVI, Segment CMR) and deformation metrics, with reproducibility assessed in a limited number of patients [28–30]. Although RA strain has shown high within-study reproducibility (intra/interobserver ICC 0.94/0.92), proposed prognostic thresholds vary substantially (≤27% and ≤16.1%), limiting their clinical standardization [31,32]. ANGIE-derived T1 mapping demonstrated high interobserver reproducibility for pre-contrast RV T1 (ICC 0.945); however, this technique is not widely available and is susceptible to partial-volume effects due to the thin RV wall [35]. 4D-flow CMR has its own technical challenges, including the restricted velocity dynamic range of conventional single-VENC acquisitions, long and potentially unpredictable acquisition times, large datasets, and manual, time-consuming, and non-standardized post-processing [48]. Prognostic validation of these novel CMR markers remains limited, particularly in TR. Also, the identification and validation of baseline CMR predictors of treatment response and reverse remodeling following transcatheter tricuspid interventions represent important areas for future research. Further technical improvement, standardized acquisition and post-processing, and prospective multicenter studies are required before these markers can be incorporated into routine risk stratification.

Myocardial T1 and ECV values are strongly protocol-dependent. Native T1 varies with field strength, vendor, and mapping sequence (e.g., MOLLI, shortened MOLLI, or saturation-recovery techniques), as well as with heart rate, and ECV additionally depends on the contrast agent, dose, timing of post-contrast acquisition, and hematocrit measurement. Site- and sequence-specific reference ranges are therefore required, and absolute values cannot be compared directly across studies. For the RV, these challenges are compounded by the thin wall, which is often comparable to or smaller than the in-plane voxel size of

conventional mapping sequences, resulting in partial-volume contamination from blood pool and epicardial fat. End-systolic acquisition [34] and high-resolution techniques such as ANGIE [35] partly mitigate this limitation but are not widely available, and similar considerations limit LGE assessment of the RV free wall. For hepatic ECV, region-of-interest placement (avoiding large vessels and artifacts), liver coverage within the mapping field of view, and contemporaneous hematocrit measurement are additional sources of variability.

Beyond the acquisition challenges noted above, 4D-flow CMR is available on a limited number of scanners, often as a research or optional sequence, requires dedicated post-processing software and expertise, and generates large datasets that are not easily integrated into routine clinical workflows. Results also depend on spatial and temporal resolution and on background phase-offset and eddy-current correction, and consensus recommendations for acquisition and analysis have only recently been updated [48]. Most 4D-flow data in PH therefore derive from specialized centers.

Finally, as this review has focused on functional TR and PH as the two dominant remodeling states, the generalizability of these indices to other RV-overload etiologies (e.g., congenital heart disease and arrhythmogenic RV cardiomyopathy) remains to be established. In addition, as a narrative review, this work did not include a systematic search or formal quality assessment, and the selection of studies may be subject to bias; in particular, several of the reviewed TR studies originate from the authors' research group and may be overrepresented relative to the broader literature.

3.5. Feasibility and Challenges of Clinical Adoption

Translating this evidence base into routine clinical use, however, requires weighing not only prognostic performance but also practical feasibility. The RV/LVvol ratio and nonischemic septal fibrosis are derived from standard cine and LGE datasets, and effective RVEF additionally requires pulmonary artery phase-contrast flow, which is commonly but not universally acquired; none requires specialized imaging sequences. However, each requires additional post-processing beyond routine ventricular assessment. RACI requires dedicated RA volumetric segmentation, which is not typically performed in standard CMR protocols. Hepatic ECV requires extending T1 mapping, increasingly standard for myocardial tissue characterization, to include the liver in the imaging field of view, along with pre- and post-contrast acquisitions, which adds modest scan time but no fundamentally new hardware or sequence.

For indices requiring additional acquisitions beyond a standard protocol (phase-contrast flow for effective RVEF and hepatic-extended T1 mapping for hepatic ECV), scan time, cost, and the need for specialized technical expertise remain practical barriers, particularly outside large academic referral centers. Many patients with advanced TR or PH have limited tolerance for prolonged CMR examinations because of dyspnea, inability to perform repeated breath holds, arrhythmias or the presence of implanted cardiac devices, all of which may compromise image quality or limit the feasibility of extended imaging protocols.

4. Conclusions

Novel CMR indices may provide complementary insights into right-heart remodeling beyond conventional volumetric and functional measures. Among these, effective RVEF and the RV/LVvol ratio currently have the most mature supporting evidence, and effective RVEF is the only index whose proposed threshold has been tested in independent external cohorts. RACI, NIsF, hepatic ECV, CMR-derived RA and RV strain, and SV/ESV are promising but are supported largely by single-center or derivation cohorts and require external validation and methodological standardization, whereas RV native T1 and ECV mapping and advanced 4D-flow hemodynamic metrics remain research tools. The proposed numerical thresholds

are population- and methodology-dependent and should not be regarded as validated clinical decision criteria. Moreover, current evidence establishes prognostic association rather than clinical utility; whether CMR-guided risk stratification improves the timing of intervention or patient outcomes has not been demonstrated and will require prospective, multicenter studies, including randomized strategy trials.

Author Contributions: Conceptualization, E.N., A.P. and O.K.K.; methodology, E.N., A.P. and O.K.K.; investigation, E.N., A.P. and O.K.K.; writing—original draft preparation, E.N., A.P. and O.K.K.; writing—review and editing, E.N., A.P., R.S.Z., E.M., J.W.W., J.K. and O.K.K.; visualization, E.N., A.P., E.M. and O.K.K.; supervision, J.W.W., J.K. and O.K.K.; project administration, O.K.K. All authors have read and agreed to the published version of the manuscript.

Funding: This research received no external funding.

Institutional Review Board Statement: Not applicable.

Informed Consent Statement: Not applicable.

Data Availability Statement: No new data were created or analyzed in this study.

Conflicts of Interest: The authors declare no conflicts of interest.

References

1. Dayer, N.; Ltaief, Z.; Liaudet, L.; Lechartier, B.; Aubert, J.-D.; Yerly, P. Pressure overload and right ventricular failure: From pathophysiology to treatment. *J. Clin. Med.* **2023**, *12*, 4722. [CrossRef] [PubMed]
2. Rako, Z.A.; Kremer, N.; Yogeswaran, A.; Richter, M.J.; Tello, K. Adaptive versus maladaptive right ventricular remodelling. *ESC Heart Fail.* **2023**, *10*, 762–775. [CrossRef] [PubMed]
3. Rosenkranz, S.; Howard, L.S.; Gomberg-Maitland, M.; Hoeper, M.M. Systemic consequences of pulmonary hypertension and right-sided heart failure. *Circulation* **2020**, *141*, 678–693. [CrossRef] [PubMed]
4. Garry, J.D.; Huang, S.; Annis, J.; Kundu, S.; Hemnes, A.; Freiberg, M.; Brittain, E.L. Incidence of right ventricular dysfunction in an echocardiographic referral cohort. *J. Am. Heart Assoc.* **2025**, *14*, e041096. [CrossRef] [PubMed]
5. Nochioka, K.; Roca, G.Q.; Claggett, B.; Biering-Sørensen, T.; Matsushita, K.; Hung, C.-L.; Solomon, S.D.; Kitzman, D.; Shah, A.M. Right ventricular function, right ventricular-pulmonary artery coupling, and heart failure risk in 4 US communities: The Atherosclerosis Risk in Communities (ARIC) study. *JAMA Cardiol.* **2018**, *3*, 939–948. [CrossRef] [PubMed]
6. Gorter, T.M.; Hoendermis, E.S.; van Veldhuisen, D.J.; Voors, A.A.; Lam, C.S.P.; Geelhoed, B.; Willems, T.P.; van Melle, J.P. Right ventricular dysfunction in heart failure with preserved ejection fraction: A systematic review and meta-analysis. *Eur. J. Heart Fail.* **2016**, *18*, 1472–1487. [CrossRef] [PubMed]
7. Kawut, S.M.; Barr, R.G.; Lima, J.A.C.; Praestgaard, A.; Johnson, W.C.; Chahal, H.; Ogunyankin, K.O.; Bristow, M.R.; Kizer, J.R.; Tandri, H.; et al. Right ventricular structure is associated with the risk of heart failure and cardiovascular death: The Multi-Ethnic Study of Atherosclerosis (MESA)—Right Ventricle Study. *Circulation* **2012**, *126*, 1681–1688. [CrossRef] [PubMed]
8. Zheng, J.; Yu, X.; Zhou, D.; Fan, M.; Lin, Z.; Chen, J. Prevalence and contributing factors associated with tricuspid regurgitation among patients underwent echocardiography assessment. *BMC Cardiovasc. Disord.* **2024**, *24*, 552. [CrossRef] [PubMed]
9. GBD 2021 Pulmonary Arterial Hypertension Collaborators. Global, regional, and national burden of pulmonary arterial hypertension, 1990–2021: A systematic analysis for the Global Burden of Disease Study 2021. *Lancet Respir. Med.* **2025**, *13*, 69–79. [CrossRef] [PubMed]
10. Zhang, R.S.; Villar-Calle, P.; Chevalier, C.; Khalique, O.; Guta, A.; Xiao, M.; Mayer, M.; Axman, R.; Krishnan, U.; Reza, M.; et al. Redefining right ventricular function: Incremental prognostic utility of effective RVEF on CMR in functional tricuspid regurgitation—A multicenter validation study. *JACC Cardiovasc. Imaging* **2026**, *19*, 810–821. [CrossRef] [PubMed]
11. Cavalcante, J.L.; Scherer, M.; Fukui, M.; Lerakis, S.; Harb, S.; Pursnani, A.; Schwartz, J.G.; Kapadia, S.; Ricciardi, M.J.; Khalique, O.; et al. Advanced Imaging Assessment of the Impact of Tricuspid Regurgitation on Cardiac Remodeling: The TRILUMINATE Pivotal Imaging Substudy. *J. Am. Coll. Cardiol.* **2025**, *85*, 250–261. [PubMed]
12. Altmayer, S.P.L.; Patel, A.R.; Addetia, K.; Gomberg-Maitland, M.; Forfia, P.R.; Han, Y. Cardiac MRI right ventricle/left ventricle (RV/LV) volume ratio improves detection of RV enlargement. *J. Magn. Reson. Imaging* **2016**, *43*, 1379–1385. [CrossRef] [PubMed]
13. Zhang, R.S.; Villar-Calle, P.; Jin, L.; Axman, R.; Falk, Z.; Reza, M.; Tsay, A.; Falco, G.; Cheng, A.; Chen, S.; et al. Prognostic value of the right ventricular-to-left ventricular volume ratio in tricuspid regurgitation. *JACC Adv.* **2025**, *4*, 101922. [CrossRef] [PubMed]

14. Gan, C.T.-J.; Lankhaar, J.-W.; Marcus, J.T.; Westerhof, N.; Marques, K.M.; Bronzwaer, J.G.F.; Boonstra, A.; Postmus, P.E.; Vonk-Noordegraaf, A. Impaired left ventricular filling due to right-to-left ventricular interaction in patients with pulmonary arterial hypertension. *Am. J. Physiol. Heart Circ. Physiol.* **2006**, *290*, H1528–H1533. [CrossRef] [PubMed]
15. Marcus, J.T.; Gan, C.T.-J.; Zwanenburg, J.J.; Boonstra, A.; Allaart, C.P.; Götte, M.J.; Vonk-Noordegraaf, A. Interventricular mechanical asynchrony in pulmonary arterial hypertension: Left-to-right delay in peak shortening is related to right ventricular overload and left ventricular underfilling. *J. Am. Coll. Cardiol.* **2008**, *51*, 750–757. [CrossRef] [PubMed]
16. Hardziyenka, M.; Campian, M.E.; Reesink, H.J.; Surie, S.; Bouma, B.J.; Groenink, M.; Klemens, C.A.; Beekman, L.; Remme, C.A.; Bresser, P.; et al. Right ventricular failure following chronic pressure overload is associated with reduction in left ventricular mass: Evidence for atrophic remodeling. *J. Am. Coll. Cardiol.* **2011**, *57*, 921–928. [CrossRef] [PubMed]
17. Zhang, R.S.; Jin, L.; Falco, G.; Axman, R.; Villar-Calle, P.; Tsay, A.; Lam, M.C.; Krishnan, U.; Cheng, A.; Han, Y.; et al. Prognostic value of the right ventricular to left ventricular volume ratio on cardiac magnetic resonance imaging in predicting adverse outcomes for adults with pulmonary hypertension. *Prog. Cardiovasc. Dis.* **2025**, *90*, 109–115. [CrossRef] [PubMed]
18. Zhang, R.S.; Falco, G.; Li, E.; Villar-Calle, P.; Reza, M.; Naami, E.; Manowitz, E.; Tawde, P.; Narasimhan, R.; Yadollahikhales, M.; et al. Right atrioventricular coupling index (RACI): A novel prognostic marker in functional tricuspid regurgitation. *Circ. Cardiovasc. Imaging* **2026**, *19*, e019813. [PubMed]
19. Villar-Calle, P.; Pai, V.; Zhang, R.S.; Reza, M.; Jin, L.; Axman, R.; Falk, Z.; Falco, G.; RoyChoudhury, A.; Chen, S.; et al. Nonischemic septal fibrosis in functional tricuspid regurgitation provides incremental stratification of adverse remodeling and prognosis. *JACC Cardiovasc. Imaging* **2025**, *18*, 959–969. [CrossRef] [PubMed]
20. Luetkens, J.A.; Klein, S.; Träber, F.; Schmeel, F.C.; Sprinkart, A.M.; Kuetting, D.L.R.; Block, W.; Uschner, F.E.; Schierwagen, R.; Hittatiya, K.; et al. Quantification of liver fibrosis at T1 and T2 mapping with extracellular volume fraction MRI: Preclinical results. *Radiology* **2018**, *288*, 748–754. [CrossRef] [PubMed]
21. Bergamaschi, L.; Arangalage, D.; Maurizi, N.; Pizzi, C.; Valgimigli, M.; Iglesias, J.F.; Landi, A.; Leo, L.A.; Eeckhout, E.; Schwitter, J.; et al. Hepatic T1 mapping as a novel cardio-hepatic axis imaging biomarker early after ST-elevation myocardial infarction. *Eur. Heart J. Cardiovasc. Imaging* **2025**, *26*, 229–238. [CrossRef] [PubMed]
22. Fortea, J.I.; Puente, Á.; Cuadrado, A.; Huelin, P.; Pellón, R.; González Sánchez, F.J.; Mayorga, M.; Cagigal, M.L.; García Carrera, I.; Cobreros, M.; et al. Congestive hepatopathy. *Int. J. Mol. Sci.* **2020**, *21*, 9420. [CrossRef] [PubMed]
23. Villar-Calle, P.; Zhang, R.S.; Naami, E.; Sewanan, L.; Reza, M.; Manowitz, E.; Chan, N.; Spincemaille, P.; Wang, Y.; Weinsaft, J.W.; et al. Hepatic extracellular volume fraction by CMR: A novel prognostic marker in tricuspid regurgitation. *Circ. Cardiovasc. Imaging* **2026**, *19*, e018988. [CrossRef] [PubMed]
24. Margonato, D.; Enriquez-Sarano, M.; Nishihara, T.; Phichaphop, A.; Cravero, E.; Wang, C.; Fukui, M.; Sorajja, P.; Lesser, J.; Schelbert, E.; et al. Quantitative identification of high-risk tricuspid regurgitation by cardiac magnetic resonance. *Circulation* **2025**, *152*, 1769–1780. [CrossRef] [PubMed]
25. Tian, H.; Wu, Q.; Wang, Z.; Zhang, Z.; Yan, Y.; Deng, Y.; Du, Y.; Yang, Z.; Li, D.; Yang, F. Enhancing Intermediate-Risk Stratification in Pulmonary Hypertension: CMR-Derived Quantification of Right Ventricular-Arterial Coupling. *Acad. Radiol.* **2026**, *33*, 2533–2541. [CrossRef] [PubMed]
26. Schmidt, R.; Orwat, S.; Kempny, A.; Schuler, P.; Radke, R.; Kahr, P.C.; Hellige, A.; Baumgartner, H.; Diller, G.-P. Value of speckle-tracking echocardiography and MRI-based feature tracking analysis in adult patients after Fontan-type palliation. *Congenit. Heart Dis.* **2014**, *9*, 397–406. [CrossRef] [PubMed]
27. Heermann, P.; Hedderich, D.M.; Paul, M.; Schülke, C.; Kroeger, J.R.; Baeßler, B.; Wichter, T.; Maintz, D.; Waltenberger, J.; Heindel, W.; et al. Biventricular myocardial strain analysis in patients with arrhythmogenic right ventricular cardiomyopathy (ARVC) using cardiovascular magnetic resonance feature tracking. *J. Cardiovasc. Magn. Reson.* **2014**, *16*, 75. [CrossRef] [PubMed]
28. de Siqueira, M.E.; Pozo, E.; Fernandes, V.R.; Sengupta, P.P.; Modesto, K.; Gupta, S.S.; Barbeito-Caamaño, C.; Narula, J.; Fuster, V.; Caixeta, A.; et al. Characterization and clinical significance of right ventricular mechanics in pulmonary hypertension evaluated with cardiovascular magnetic resonance feature tracking. *J. Cardiovasc. Magn. Reson.* **2016**, *18*, 39. [CrossRef] [PubMed]
29. Tello, K.; Dalmer, A.; Vanderpool, R.; Ghofrani, H.A.; Naeije, R.; Roller, F.; Seeger, W.; Wilhelm, J.; Gall, H.; Richter, M.J. Cardiac Magnetic Resonance Imaging-Based Right Ventricular Strain Analysis for Assessment of Coupling and Diastolic Function in Pulmonary Hypertension. *JACC Cardiovasc. Imaging* **2019**, *12*, 2155–2164. [CrossRef] [PubMed]
30. Romano, S.; Dell'Atti, D.; Judd, R.M.; Kim, R.J.; Weinsaft, J.W.; Kim, J.; Heitner, J.F.; Hahn, R.T.; Farzaneh-Far, A. Prognostic Value of Feature-Tracking Right Ventricular Longitudinal Strain in Severe Functional Tricuspid Regurgitation: A Multicenter Study. *JACC Cardiovasc. Imaging* **2021**, *14*, 1561–1568. [CrossRef] [PubMed]
31. Yang, F.; Yan, Y.; Jiang, W.; Wang, Z.; Wu, C.; Wu, Q.; Deng, Y.; Du, Y.; Yang, Z.; Zhang, Z.; et al. Impaired right atrial function preceding right ventricular systolic dysfunction: Clinical utility and long-term prognostic value in pulmonary hypertension. *Insights Imaging* **2025**, *16*, 115. [CrossRef] [PubMed]
32. Guo, J.; Leng, S.; He, J.; Yin, L.; Chen, C.; Liu, X.; Zhao, J.; Wan, K.; Wang, J.; Xu, Y.; et al. Right atrial phasic strain in risk stratification of patients with Pulmonary Arterial Hypertension. *J. Cardiovasc. Magn. Reson.* **2026**, 102711. [CrossRef] [PubMed]

33. Kim, J.; Son, J.; Kim, O.; Choi, K.H.; Yang, J.H.; Kim, E.K.; Chang, S.-A.; Lee, S.-C.; Park, S.W.; Kim, S.M.; et al. Noninvasive estimation of right atrial pressure using cardiac magnetic resonance in severe tricuspid regurgitation. *J. Cardiovasc. Magn. Reson.* **2026**, *28*, 102710. [CrossRef] [PubMed]
34. Asano, R.; Ogo, T.; Morita, Y.; Kotoku, A.; Aoki, T.; Hirakawa, K.; Nakayama, S.; Ueda, J.; Tsuji, A.; Waddingham, M.T.; et al. Prognostic value of right ventricular native T1 mapping in pulmonary arterial hypertension. *PLoS ONE* **2021**, *16*, e0260456. [CrossRef] [PubMed]
35. Mehta, B.B.; Auger, D.A.; Gonzalez, J.A.; Workman, V.; Chen, X.; Chow, K.; Stump, C.J.; Mazimba, S.; Kennedy, J.L.W.; Gay, E.; et al. Detection of elevated right ventricular extracellular volume in pulmonary hypertension using Accelerated and Navigator-Gated Look-Locker Imaging for Cardiac T1 Estimation (ANGIE) cardiovascular magnetic resonance. *J. Cardiovasc. Magn. Reson.* **2015**, *17*, 110. [CrossRef] [PubMed]
36. Goh, Z.M.; Balasubramanian, N.; Alabed, S.; Dwivedi, K.; Shahin, Y.; Rothman, A.M.K.; Garg, P.; Lawrie, A.; Capener, D.; Thompson, A.A.R.; et al. Right ventricular remodelling in pulmonary arterial hypertension predicts treatment response. *Heart* **2022**, *108*, 1392–1400. [CrossRef] [PubMed]
37. Celant, L.R.; Wessels, J.N.; Kianzad, A.; Marcus, J.T.; Meijboom, L.J.; Bogaard, H.J.; de Man, F.S.; Noordegraaf, A.V. Restoration of right ventricular function in the treatment of pulmonary arterial hypertension. *Heart* **2023**, *109*, 1844–1850. [CrossRef] [PubMed]
38. Rischard, F.P.; Bernardo, R.J.; Vanderpool, R.R.; Kwon, D.H.; Acharya, T.; Park, M.M.; Katrynuik, A.; Insel, M.; Kubba, S.; Badagliacca, R.; et al. Classification and Predictors of Right Ventricular Functional Recovery in Pulmonary Arterial Hypertension. *Circ. Heart Fail.* **2023**, *16*, e010555. [CrossRef] [PubMed]
39. Ota, H.; Kamada, H.; Higuchi, S.; Takase, K. Clinical Application of 4D Flow MR Imaging to Pulmonary Hypertension. *Magn. Reson. Med. Sci.* **2022**, *21*, 309–318. [CrossRef] [PubMed]
40. Reiter, G.; Reiter, U.; Kovacs, G.; Olschewski, H.; Fuchsjäger, M. Blood flow vortices along the main pulmonary artery measured with MR imaging for diagnosis of pulmonary hypertension. *Radiology* **2015**, *275*, 71–79. [CrossRef] [PubMed]
41. Kim, B.; Lee, J.; Berhane, H.; Freed, B.H.; Shah, S.J.; Thomas, J.D. Differences in Pulmonary Artery Flow Hemodynamics Between PAH and PH-HFpEF: Insights From 4D-Flow CMR. *Pulm. Circ.* **2025**, *15*, e70022. [CrossRef] [PubMed]
42. Dong, M.L.; Azarine, A.; Haddad, F.; Amsallem, M.; Kim, Y.W.; Yang, W.; Fadel, E.; Aubrege, L.; Loecher, M.; Ennis, D.; et al. 4D flow cardiovascular magnetic resonance recovery profiles following pulmonary endarterectomy in chronic thromboembolic pulmonary hypertension. *J. Cardiovasc. Magn. Reson.* **2022**, *24*, 59. [CrossRef] [PubMed]
43. Rahgozar, K.; Bruoha, S.; Ho, E.; Goldberg, Y.; Chau, M.; Latib, A. Rediscovered and unforgotten: Transcatheter interventions for the treatment of severe tricuspid valve regurgitation. *US Cardiol. Rev.* **2021**, *15*, e22. [CrossRef] [PubMed]
44. Ehrenfels, M.A.; Fretter, C.; von Stein, J.; Körber, M.I.; Wienemann, H.; Baldus, S.; Pfister, R.; Iliadis, C. Role of preexisting right ventricular remodeling in symptoms and prognosis after transcatheter tricuspid valve repair. *Clin. Res. Cardiol.* **2024**, *114*, 187–202. [CrossRef] [PubMed]
45. Kim, J.; Srinivasan, A.; Seoane, T.; Di Franco, A.; Peskin, C.S.; McQueen, D.M.; Paul, T.K.; Feher, A.; Geevarghese, A.; Rozenstrauch, M.; et al. Echocardiographic linear dimensions for assessment of right ventricular chamber volume as demonstrated by cardiac magnetic resonance. *J. Am. Soc. Echocardiogr.* **2016**, *29*, 861–870. [CrossRef] [PubMed]
46. Kochav, J.; Chen, J.; Nambiar, L.; Mitlak, H.W.; Kushman, A.; Sultana, R.; Horn, E.; RoyChoudhury, A.; Devereux, R.B.; Weinsaft, J.W.; et al. Novel echocardiographic algorithm for right ventricular mass quantification: Cardiovascular magnetic resonance and clinical prognosis validation. *J. Am. Soc. Echocardiogr.* **2021**, *34*, 839–850.e1. [CrossRef] [PubMed]
47. Fine, N.M.; Tandon, S.; Kim, H.W.; Shah, D.J.; Thompson, T.; Drangova, M.; White, J.A. Validation of sub-segmental visual scoring for the quantification of ischemic and nonischemic myocardial fibrosis using late gadolinium enhancement MRI. *J. Magn. Reson. Imaging* **2013**, *38*, 1369–1376. [CrossRef] [PubMed]
48. Bissell, M.M.; Raimondi, F.; Ali, L.A.; Allen, B.D.; Barker, A.J.; Bolger, A.; Burris, N.; Carhäll, C.-J.; Collins, J.D.; Ebbers, T.; et al. 4D Flow cardiovascular magnetic resonance consensus statement: 2023 update. *J. Cardiovasc. Magn. Reson.* **2023**, *25*, 40. [CrossRef] [PubMed]

Disclaimer/Publisher's Note: The statements, opinions and data contained in all publications are solely those of the individual author(s) and contributor(s) and not of MDPI and/or the editor(s). MDPI and/or the editor(s) disclaim responsibility for any injury to people or property resulting from any ideas, methods, instructions or products referred to in the content.